Comprehensive clinicopathological and molecular analysis of primary malignant melanoma of the oesophagus

Sho, Tsuyama MD[1)]; Shinji, Kohsaka, MD, PhD[2)]; Takuo, Hayashi, MD, PhD[1)]; Yoshiyuki, Suehara, MD, PhD[3), 4)]; Takashi, Hashimoto, MD, PhD[5)]; Yoshiaki, Kajiyama, MD, PhD[5)]; Masahiko, Tsurumaru MD, PhD[5)]; Toshihide, Ueno, PhD[2)]; Hiroyuki, Mano, MD, PhD[2)]; Takashi, Yao MD, PhD[1)]; Tsuyoshi, Saito MD, PhD[1), 3)]

1) Department of Human Pathology, Juntendo University Graduate School of Medicine, Tokyo 113-8421, Japan

2) Division of Cellular Signaling, National Cancer Center Research Institute, Tokyo 104-0045, Japan

3) Intractable Disease Research Center, Juntendo University, Graduate School of Medicine, Tokyo 113-8421, Japan

4) Department of Orthopaedic Surgery, Juntendo University School of Medicine, Tokyo 113-8421, Japan

5) Department of Esophageal and Gastroenterological Surgery, Juntendo University School of Medicine, Tokyo 113-8421, Japan

Corresponding author: Tsuyoshi Saito, MD, PhD

Address: Hongo 2-1-1, Bunkyo-ku, Tokyo, Japan 113-8421

TEL +81-3-5802-1037

FAX +81-3-3812-1056

E-mail: tysaitou@juntendo.ac.jp.

Running title: Genetic alterations in melanoma of the oesophagus

Conflict of interest

The authors declare no conflict of interest.

Funding information

This study was financially supported in part through grants from the Program for Integrated Database of Clinical and Genomic Information under Grant Number JP18kk0205003, the Practical Research for Innovative Cancer Control under Grant Number JP18ck0106252, and the Project for Cancer Research And Therapeutic Evolution (P-CREATE) under Grant Number JP18cm0106502 from the Japan Agency for Medical Research and Development, AMED. This study was financially supported in part by a Grant-in-Aid for General Scientific Research from the Ministry of Education, Science, Sports, and Culture (#17K08704 to Takashi Yao, and #17K08730 to Tsuyoshi Saito), Tokyo, Japan. This research was supported by AMED under Grant Number JP17am0001009. This study was also supported by Grant for Cross-disciplinary Collaboration, Juntendo University (30-18).

Abstract

Aims: This study was performed to elucidate the clinicopathological characteristics, genetic alterations, and therapeutic targets of primary malignant melanoma of the oesophagus (PMME). **Methods**: The clinicopathology and molecular pathology of 13 PMME and 10 skin malignant melanoma (SKMM) cases were analysed via next-generation sequencing (NGS) and immunohistochemistry. **Results**: Three-year overall survival rate and the median survival time for PMME patients were 23.1% and 11.9 months, respectively. Three (23.1%) and eight (61.5%) PMME cases exhibited a papillary structure and lymph node metastasis, respectively. DNA and RNA hybridisation capture-based NGS analysis revealed that *NF1* was the most frequently mutated gene (30%) in 10 of the PMME cases. Other mutations detected in PMME included *SF3B1* (20%), *KRAS* (10%), *BRCA2* (10%), *KIT* (10%), and *TP53* (10%). Commonly detected *BRAF* mutations in SKMM were not detected in PMME. Immunohistochemistry and mutation status were concordant between p53/c-kit and *TP53/KIT*, respectively. Focal expression of PD-L1 was observed in one PMME sample. The tumour mutation burden in PMME was significantly lower than that in SKMM (p = 0.030). No PMME case displayed high microsatellite instability. RNA-sequencing revealed a distinctive pattern with respect to RNA expression. T-cell co-stimulation differed between PMME and SKMM. **Conclusions**: The RAS-MAPK pathway is one of the main pathways involved in PMME. The genetic profile of PMME was similar to that of mucosal/acral melanoma but differed from the SKMM profile. A subset of PMME may contain actionable mutations. Immunotherapy seemed to be less effective for most PMMEs in this series.

Key words: primary malignant melanoma of the oesophagus (PMME); molecular pathogenesis; next-generation sequencing (NGS); immunotherapy; tumour mutation burden (TMB)

1. Background

Malignant melanomas have been historically classified into several subtypes based on the tissue from which the primary tumour arises. The major subtypes are cutaneous melanoma (CM), which arises in non-glabrous skin; acral melanoma (AM), a distinct form that originates in the glabrous skin of the palms, soles and nail beds; mucosal melanoma (MM), which arises from melanocytes in the mucosa lining internal tissues and uveal melanoma (UM), which develops from melanocytes in the uveal tract of the eye [1]. Among these subtypes, primary malignant melanoma of the oesophagus (PMME) is an extremely rare cancer of the oesophagus, accounting for 0.1–0.8% of oesophageal cancers and <0.05% of all melanoma subtypes [2,3]. The malignant melanoma of the oesophagus was first proposed by Baur in 1906 [4]. Since the first case and up to 2014, 369 cases of PMME have been reported [5,6]. PMME comprises 5.6% of all gastrointestinal (GI) tract melanomas [7]. Although PMME is a rare subtype of oesophageal cancer, it has been relatively well reviewed [5,6,8-10]. PMME is a highly aggressive tumour that is associated with a poor prognosis [6,8-11].

With respect to the molecular pathogenesis of these tumours, the genetics of CM has been well studied. CMs are genetically classified as *BRAF*-mutant (50%), *RAS*-mutant (20–30%), *NF1*-mutant (10%–15%), or triple wild-type (10%–15%) [12]. Identification of several active molecular aberrations, such as *BRAF*^{V600} mutations, has resulted in molecular targeted therapy with BRAF and MEK inhibitors in patients with CM and has contributed to the improved prognosis [13,14]. Recent genetic studies have also focused on less frequent melanoma subtypes, such as AM, as well as PMME [10,15-18]. Hayward et al. reported that

AM was associated with more frequent chromosomal alterations and a lower tumour mutation burden (TMB) than non-acral skin melanoma [19]. In AM, *NF1* and *KIT* mutations are more frequent compared to CM [19]. Previous studies have revealed the genetic features of MM [20,21]. However, the molecular pathogenesis of PMME remains unclear. Furthermore, the prognosis of patients with PMME remains poor because of its high metastatic potential, despite multimodal therapies that include radical surgery with chemotherapy, chemoradiotherapy, immunotherapy or other adjuvant therapies.[22]

This study was performed to elucidate the genetic alterations and pathogenesis of PMME by next-generation sequencing (NGS) in addition to clinicopathological analysis to identify novel therapeutic targets. The findings may lead to an improved prognosis of PMME.

2. Materials & Methods

2.1. Patient and tissue samples

Thirteen cases of PMME and 10 cases of skin malignant melanoma (SKMM) were collected from pathological files at Juntendo University Hospital from 2003 to 2016. We reconfirmed the diagnosis of PMMEs as the existence of focal adjacent junctional melanocytic activity or melanoma *in situ*, and the absence of melanoma in any other skin, mucosal (anorectum, nasal and oral cavity, oral pharynx), or ocular origin [5]. SKMMs were defined as both CM and AM [1]. Macroscopic features were classified according to the criteria proposed by the Japan Esophageal Society. Type 0-I is a superficial and protruded type that is subclassified as Type 0-Ip (pedunculated lesion) and type 0-Is (sessile lesion). Type 0-II is a superficial and flat type that is subclassified as Type 0-IIa+IIc, which is a slightly elevated and depressed type. There were five types of advanced tumours, with Type 1 being a protruding type and Type 5 being unclassified [23]. This macroscopic classification also referred to the World Health Organisation classification [24]. Pathological staging of tumours was made in accordance with the Tumour Node Metastasis (TNM) classification of the eighth edition of the Union for International Cancer Control classification of malignant tumours [25]. The surgical specimens were fixed in 10% buffered formalin, embedded in paraffin, and stained with haematoxylin and eosin (H&E). The presence of the following features (regardless of the proportion) was evaluated: epithelioid with/without rhabdoid feature, papillary type, and spindle type (Fig. 1). This study was approved by the Ethical Committee of Juntendo University School of Medicine, Tokyo, Japan (2016-108, 2017-139).

2.2. NGS DNA-seq by TOP panel

DNA was extracted from the tumoural and non-tumoural tissues of all patients. DNA extraction from formalin-fixed, paraffin-embedded (FFPE) tissues, was performed using the Maxwell nucleic extractor (Promega, Italia S.R.L, Milan, Italy). NGS was performed using the Todai OncoPanel (TOP), which is a DNA and RNA hybridisation capture-based NGS panel [26]. Mutations with <10% allele frequency were determined.

2.3. RNA-seq analysis

Total RNA was extracted from tumour FFPE samples using an RNeasy FFPE Kit (Qiagen, Valencia, CA, USA) and treated with DNase I (Thermo Fisher Scientific, Waltham, MA, USA). cDNA synthesis and library preparation for coding exon capture were performed using the TruSight RNA Pan-Cancer Panel (Illumina, San Diego, CA, USA), according to the manufacturer's protocol. TOP RNA panel v5 was used. RNA expression analysis was performed by TopHat v2.0.9 and cufflinks v2.1.1 after quality control (Trim Galore!; Babraham Informatics, https://www.bioinformatics.babraham.ac.uk/projects/trim_galore/). The RNA expression data were analysed using cluster analysis.

2.4. Immunohistochemistry (IHC)

IHC was performed using the indirect polymer method with the Envision™ system (DAKO Cytomation, Glostrup, Denmark). Details of the primary antibodies and conditions used in this research purpose are summarised in Table 1. Immunohistochemistry using S-100, HMB-45, and Melan A were also performed in the routine diagnostic process (Supplementary Table 2). Programmed death ligand 1 (PD-L1) staining (22C3, DAKO Cytomation) was also

performed on a tissue microarray (TMA). Nuclear staining was performed by Giemsa stain in all cases. Immunohistochemical staining results were evaluated by two pathologists (S.T. and T.S.).

2.5. Microsatellite instability (MSI) analysis

DNA was extracted from tumour and normal tissues by microdissection. If two or more of the five microsatellite sequences in the National Cancer Institute recommended panel of microsatellites (Supplementary Table 1) in the tumour DNA were mutated, the tumour was termed MSI-high (MSI-H). If only one of the five microsatellite sequences in the tumour DNA was mutated, the tumour was termed MSI-low (MSI-L). If none of the five microsatellite sequences in the tumour DNA was mutated, the tumour was termed microsatellite stable (MSS) [27].

2.6. Statistical analysis

All data differences are considered significant at $P < 0.05$. Survival analysis was performed according to the Kaplan-Meier method. The statistical analysis was performed with R (The R Foundation for Statistical Computing, Vienna, Austria) and EZR (Saitama Medical Center, Jichi Medical University, Saitama, Japan), which is a graphical user interface for R.

3. Results

3.1. Clinicopathological characteristics

In Juntendo University Hospital, oesophageal surgical resections were performed in 1720 cases from 2003 to 2016. The incidence of PMME was 13/1720 (0.76%). The clinicopathological findings of PMME are summarised in Table 2. Detailed findings in PMME and SKMM are summarised in Supplementary Table 2-1, 2-2 and Supplementary Table 3, respectively. Regarding PMME, the mean patient age was 63.2 years (range 47–74 years). The male-to-female ratio was 11:2 (84.6%:15.4%). Tumour location was restricted in the middle to lower oesophagus, except for one case (Supplementary Table 2-1). Seven cases (53.8%) were located in the middle portion, 5 cases (38.5%) were located in the lower third portion or esophago-gastric junction, and one case (7.7%) was located in the upper portion.

Macroscopically and histologically, all tumours exhibited protruded lesions. Eight cases were classified as Type 0-I (0-Ip, n = 6 and 0-Is, n = 2), one case as Type 0-IIa+IIc, 3 cases as Type 1 and one case as Type 5. The mean tumour size was 40.3 mm (range 21–58 mm). All cases had melanin pigmentation, 12 cases exhibited melanoma *in situ* or junctional activity, and 12 cases featured melanocytosis. The melanoma *in situ* lesion could not be confirmed in one case (PMME #10). However, the oesophagus was regarded as the primary site since no other possible primary lesion or past clinical history of malignant melanoma was noted. In addition, this case showed an ulcered and well circumscribed lesion, like a submucosal tumour. The *in situ* lesion might have disappeared due to ulcer formation in this case. There was intramucosal invasion (M) in one case, submucosal invasion (SM) in 7 cases and invasion

to muscularis propria (MP) in 5 cases. Lymph node metastasis was observed in 8 of the 13 cases (61.5%). Regarding the association with invasion depth, lymph node metastasis was positive for one in the tumour restricted to mucosa, in 3 of 7 tumours with invasion to submucosa and in 4 of 5 tumours with invasion to the MP. Morphologically, the epithelioid type with rhabdoid feature was apparent in 6 cases, the epithelioid type without rhabdoid feature in 5 cases, the papillary type in 3 cases and the spindle type in 2 cases.

Distant metastasis was noted in 12 of the 13 cases (92.3%) post-surgery. Only one the patient without distant metastasis displayed prolonged survival. The most common distant metastatic sites were the lung and abdomen (3/13), followed by bone, liver, pleura, skin (2/13), and the adrenal gland and eye (1/13). Cases #4 and #8-10 received neoadjuvant therapy. Five cases received chemotherapy after surgical treatment. Case #13 received immunotherapy with the PD-L1 inhibiter Nivolumab after surgery. This patient died of the disease 40 days after treatment.

3.2. IHC

IHC analysis revealed overexpression of p53 in one of the 13 cases (7.7%, case #12). C-kit was positive in one case (7.7%, case #11). Both cases were concordant with genetic mutations (Fig. 2). All cases were negative for the cytokeratins CAM5.2, AE1/AE3, and epithelial membrane antigen. PD-L1 IHC was positive for case 10 of PMME. The remaining cases were negative. PD-L1 IHC was positive for only one case from SKMM (case #9).

3.3. Survival analysis

Twelve patients (92.3%) had died of the disease and one patient (case #5) had been lost to follow-up after approximately 12 years of follow-up. Relapse-free survival rates were 23.1% (1 year), 23.1% (3 years), and 7.7% (5 years) (Fig. 3A). Overall survival rates were 46.2% (1 year), 23.1% (3 years), and 7.7% (5 years) (Fig. 3B). The mean survival period was 29.8 months (range 5.5–152.4), and the median overall survival rate was 11.9 months (95% confidence interval 7.3–36). The patient who survived for more than 10 years (case #5) had a superficial tumour, and no lymphovascular invasion or no lymph node metastasis, despite submucosa invasion. Three- and five-year overall survival rates of the patients without lymph node metastasis at surgery were 40% and 20%, respectively. Overall, survival tended to be better for patients with papillary structure and *NF1* mutation, although these data were not significant (Supplementary Fig. 1A and 1B: $p = 0.173$, $p = 0.252$, respectively).

3.4 Genetic alterations

NGS data were obtained for 10 of 13 patients with PMME. Insufficient reads were obtained from the remaining 3 cases due to poor sample quality. Table 3 summarises the data for genetic alterations with IHC findings. DNA analysis revealed that *NF1* was the most frequently mutated gene in PMME (3/10 cases, 30%), followed by *SF3B1* mutation (2/10, 20%). *KRAS, KIT, BRCA2, TP53,* and *CDKN2A* mutations were found in one case each (1/10, 10%). No *BRAF* mutation was detected. In contrast, DNA analysis was successful for 9 cases of SKMM (Supplementary Table 4). *BRAF* (V600E) and *NF1* mutations were detected in 4 cases (44.4%) and 3 cases (33%) of SKMM, respectively. Tumour mutation burden (TMB) in PMME was significantly lower than that in SKMM (Fig. 4, $p = 0.0303$, Mann–Whitney U test). All patients with PMME were MSS or MSI-L (Table 3).

3.5. Gene expression analysis

Supervised cluster analysis was performed using the list of the top 100 differentially expressed genes, (Fig. 5). This analysis clearly discriminated PMME and SKMM, except for SKMM#1, suggesting that PMME is a distinctive tumour from SKMM. Furthermore, supervised analysis based on the expression data of costimulatory and coinhibitory receptors involved in the immunoreaction [28] separated the two groups. Both cases with PD-L1 expression (PMME #10 and SKMM #9) clustered within the same group with higher expression of immune reaction-related genes (Fig. 6). Interestingly, there was no relationship between TMB and the expression level of immune reaction-related genes. Furthermore, fusion genes including *EWSR1-CREB1* and *EWSR1-ATF1,* which are found in clear cell sarcoma-like tumours of the GI tract, were not detected by fusion gene analysis in RNA-seq.

4. Discussion

The prognosis in PMME was previously considered to be extremely poor. Tumour size, depth, stage, and lymph node metastasis were not prognostic factors in this study. However, a recent study reported that patients with long-term survival had PMME that had reached the submucosa but not metastasised to the lymph nodes [10]. In addition, a review of 134 patients with malignant melanoma of the oesophagus over a 10-year period from 1998 to 2007 indicated that the tumour stage and lymph node metastasis were prognostic factors for PMMEs [6]. In this study, one case (PMME #5) with good prognosis did not display nodal metastasis at the time of surgery. However, PMME #4 had muscularis mucosae invasion, but had lymph node metastasis accompanied by lymphovascular invasion, which led to a poor prognosis. This discrepancy may have reflected the smaller sample size of our study.

PMME can be morphologically divided into an epithelioid pattern with/without rhabdoid feature, a spindle pattern, and a papillary pattern. The prognosis was better for the papillary pattern of PMME (Supplementary Fig. 1A), although the difference was not statistically significant. This finding might suggest PMME with a papillary structure can be well-differentiated in terms of biological behaviour, although a larger sample size is necessary to confirm this suggestion.

Targeted exon sequencing analysis of 15 cases of anorectal melanoma revealed some recurrent pathogenic mutations that included *KIT, SF3B1, TP53, NF1, RAS, BRAF, MLH1* and *BRCA1* [29]. Interestingly, these mutations were reflective of the mutation status in the present study. These findings may imply that the tumorigenesis of PMME is the same as that of anorectal melanoma, even though they are genetically heterogeneous entities.

A previous study reported frequent *NRAS* mutations (6/16, 37.5%) but infrequent *BRAF* mutations (1/16, 6.25%) in PMME [18]. Another recent study demonstrated *NRAS* mutation in 33% (5/15) of PMME and *BRAF* mutation in none of the cases [10]. In this study, we did not detect a *BRAF* mutation in any of cases and detected a *KRAS* mutation, but not *NRAS* mutation, in only one case (10%). Infrequent *BRAF* mutation seemed to be consistent in previous studies. However, the lower frequency of *RAS* mutations in this study seemed to be inconsistent.

This study identified for the first time that *NF1* mutation was the most frequent mutation in PMME (30%), although a recent NGS study failed to detect the *NF1* mutation, since the cancer hotspot panel used in that study lacked the *NF1* gene [10]. *NF1* is a tumour suppressor gene that encodes the RAS GTPase-activation protein (RAS GAP) neurofibromin, which negatively regulates RAS by catalysing the hydrolysis of RAS-GTP to RAS-GDP. Generally, NF1 is a GTPase activating protein that downregulates the activity of the RAS protein. Consequently, loss of function mutations in *NF1* are important genetic mechanisms underlying constitutive activation of the mitogen-activated protein kinase (MAPK) pathway [12]. The involvement of *NF1* mutation in melanomagenesis has been demonstrated [30] and the involvement of *NF1* and *KIT* mutations in MM have been shown by whole-exome sequencing [31]. Based on these findings, trametinib or cobimetinib, which inhibits MARK kinase (MEK), could be useful in the treatment of *NF1* mutated PMME [32].

SF3B1 is a part of the U2 small nuclear ribonucleoprotein complex that participates in pre-mRNA splicing [33]. Two cases of PMME harboured the same R625H mutation, which is a

common mutation found in UM, anorectal melanoma, adenoid cystic carcinoma, and chronic lymphocytic leukaemia [34]. As new therapeutic agents have been developed for *SF3B1* mutated tumours, in the future there may be various treatment options for PMME with mutation of *SF3B1*.

A *KIT* mutation was found in PMME case #11 with c-kit expression. This finding is consistent with previous studies in which IHC helped to detect *KIT*-positive melanomas [18,35,36]. In general, melanocytes express c-kit. Therefore c-kit-positive melanoma probably preserves the character of melanocytes, leading to the hypothesis that c-kit-positive melanoma is a well-differentiated tumour [37]. The tyrosine kinase inhibitor Imatinib is reportedly effective for some *KIT*-positive melanomas [38,39]. However, the *KIT* mutation found in PMME case #11 was a p.Asn822Tyr (N822Y) mutation. A secondary mutation associated with acquired resistance to Imatinib occurs at this position. Therefore, Imatinib might be less effective in this case, as melanomas with *KIT* mutations that involve the distal kinase domain are less affected by Imatinib [40].

BRCA1/2 mutations are associated with DNA damage repair. Tumours with *BRCA2* mutations respond to poly(ADP-ribose) polymerase inhibitors. These inhibitors are recommended for the treatment of breast cancer harbouring the *BRCA1/2* mutations [41]. The *BRCA1/2* mutations might be potential therapeutic targets in PMME.

TMB in PMME was significantly lower than that of SKMM (Fig. 4; $p = 0.0303$). TMB correlates well with the response to immunotherapy in many cancers [42]. In PMME #1, TMB was extremely high among the PMME group. This patient died of the disease 5.5 months

after surgery, despite submucosal invasion without lymph node metastasis. In non-small cell lung cancer, the prognostic significance of higher TMB is controversial [43,44], although its impact on patients with MM has not been well described [45]. Supervised analyses based on the expression data of costimulatory and coinhibitory receptors involved in the immunoreaction separated the two groups. In this study, IHC revealed PD-L1 expression in two cases (PMME #10 and SKMM #9). The potential effect of immunotherapy for these two patients is unknown, because they did not receive immunotherapy. One patient (PMME #13) from a group with lower immunoreaction-related expression, was treated with Nivolumab. However, there was no effect. In addition, TMB and expression of immunoreaction-related genes did not corelate in the PMME and SKMM cases, although all PMME cases were MSS or MSI-L by MSI analysis.

Finally, clear cell sarcoma and clear cell sarcoma-like tumour of the GI tract could be the main features of the differential diagnosis of PMME. These tumours harbour *EWSR1-ATF1* and *EWSR1-CREB1* fusion genes. However, *EWSR1-ATF1* and *EWSR1-CREB1* fusions were not detected in any of the present PMME cases, suggesting that PMME is a distinct tumour within the tumour spectra.

In conclusion, PMME harboured some characteristic genetic mutations. The *NF1* mutation was the most frequent, followed by *SF3B1, KIT, TP53, KRAS* and *BRCA2*. Some of these may be actionable mutations. The genetic profile of PMME was almost the same as MM/AM, but was different from that of SKMM. The findings indicate that immunotherapy may be less effective for most PMMEs.

Acknowledgements

We thank Noriko Sasahara, Isao Kurahayashi, Satomi Saito, Chisato Kohara, Hiroshi Sonoue, and Katsunobu Yamasato for their excellent technical assistance. We also thank the Laboratory of Molecular and Biochemical Research, Research Support Center, Juntendo University Graduate School of Medicine, for technical assistance.

Author contributions statement

ST, TS, TH, YS, and TY planned this project. ST, TS, TH, and TY contributed to the diagnoses of melanoma cases. ST, TS, TH, YS, TU, and SK performed the main parts of the experiments. ST, TS, TH, YS, TU, SK, and HM analysed the data. ST and TS wrote the majority of the manuscript. TH, YK, and MT provided melanoma samples and clinical data.

References

1. Rabbie R, Ferguson P, Molina-Aguilar C, Adams DJ, Robles-Espinoza CD. Melanoma subtypes: genomic profiles, prognostic molecular markers and therapeutic possibilities. J Pathol 2019; 247: 539-551.

2. Cote TR, Sobin LH. Primary melanomas of the esophagus and anorectum: epidemiologic comparison with melanoma of the skin. Melanoma Res 2009; 19: 58-60.

3. Tachimori Y, Ozawa S, Numasaki H, et al. Comprehensive registry of esophageal cancer in Japan, 2012. Esophagus: official journal of the Japan Esophageal Society 2019; 16: 221-245.

4. Bauer, E.H.: Ein Fall von primarem Melanom des Osopagus. *Arb pathol AnatInst Tubingen.* 1906; 5: 343.

5. Bisceglia M, Perri F, Tucci A, et al. Primary malignant melanoma of the esophagus: a clinicopathologic study of a case with comprehensive literature review. Adv Anat Pathol 2011; 18: 235-252.

6. Makuuchi H, Takubo K, Yanagisawa A, Yamamoto S. Esophageal malignant melanoma: analysis of 134 cases collected by the Japan Esophageal Society. Esophagus: official journal of the Japan Esophageal Society 2015; 12: 158-169.

7. Cheung MC, Perez EA, Molina MA, Jin X, Gutierrez JC, Franceschi D, et al. Defining the role of surgery for primary gastrointestinal tract melanoma. J Gastrointest Surg. 2008;12(4):731-8.

8. Volpin E, Sauvanet A, Couvelard A, Belghiti J. Primary malignant melanoma of the esophagus: a case report and review of the literature. Dis Esophagus 2002; 15: 244-249.9.

9. Gao S, Li J, Feng X, Shi S, He J. Characteristics and Surgical Outcomes for Primary Malignant Melanoma of the Esophagus. Sci Rep 2016; 6: 23804.

10. Lasota J, Kowalik A, Felisiak-Golabek A, et al. Primary malignant melanoma of esophagus: clinicopathologic characterization of 20 cases including molecular genetic profiling of 15 tumors. Mod Pathol 2019; 32: 957-966.

11. Caldwell CB, Bains MS, Burt M. Unusual malignant neoplasms of the esophagus. Oat cell carcinoma, melanoma, and sarcoma. J Thorac Cardiovasc Surg 1991; 101: 100-107.

12. Genomic Classification of Cutaneous Melanoma. Cell 2015; 161: 1681-1696.

13. Dummer R, Ascierto PA, Gogas HJ, et al. Overall survival in patients with BRAF-mutant melanoma receiving encorafenib plus binimetinib versus vemurafenib or encorafenib (COLUMBUS): a multicentre, open-label, randomised, phase 3 trial. Lancet Oncol 2018; 19: 1315-1327.

14. Nakamura Y, Asai J, Igaki H, et al. Japanese Dermatological Association Guidelines: Outlines of guidelines for cutaneous melanoma 2019. J Dermatol 2019.

15. Haugh AM, Zhang B, Quan VL, et al. Distinct Patterns of Acral Melanoma Based on Site and Relative Sun Exposure. J Invest Dermatol 2018; 138: 384-393.

16. Langer R, Becker K, Feith M, Friess H, Hofler H, Keller G. Genetic aberrations in primary esophageal melanomas: molecular analysis of c-KIT, PDGFR, KRAS, NRAS and BRAF in a series of 10 cases. Mod Pathol 2011; 24: 495-501.

17. Terada T. Amelanotic malignant melanoma of the esophagus: report of two cases with immunohistochemical and molecular genetic study of KIT and PDGFRA. World J

Gastroenterol 2009; 15: 2679-2683.

18. Sekine S, Nakanishi Y, Ogawa R, Kouda S, Kanai Y. Esophageal melanomas harbor frequent NRAS mutations unlike melanomas of other mucosal sites. Virchows Arch 2009; 454: 513-517.

19. Hayward NK, Wilmott JS, Waddell N, et al. Whole-genome landscapes of major melanoma subtypes. Nature 2017; 545: 175-180.

20. Newell F, Kong Y, Wilmott JS, Johansson PA, Ferguson PM, Cui C, et al. Whole-genome landscape of mucosal melanoma reveals diverse drivers and therapeutic targets. Nature communications. 2019;10(1):3163.

21. Wong K, van der Weyden L, Schott CR, Foote A, Constantino-Casas F, Smith S, et al. Cross-species genomic landscape comparison of human mucosal melanoma with canine oral and equine melanoma. Nature communications. 2019;10(1):353.

22. Iwanuma Y, Tomita N, Amano T, et al. Current status of primary malignant melanoma of the esophagus: clinical features, pathology, management and prognosis. J Gastroenterol 2012; 47: 21-28.

23. Esophageal Society J. Japanese Classification of Esophageal Cancer, 11th Edition: part I. Esophagus: official journal of the Japan Esophageal Society 2017; 14: 1-36.

24. Brown IS, Fujii S, Kawachi H, Lam AK, Saito T: WHO classification of tumors of the digestive system. 5th ed. WHO Classification of Tumours Editorial Board, editors Lyon: IARC; 2019, p. 50-51.

25. TNM Classification of Malignant Tumours. 8th ed, (Brierley, JD., Gospodarowicz, MK., Wittekind, Ch, editors) Oxford, John Wiley & Sons Inc; 2017, p.55-62.

26. Kohsaka S, Tatsuno K, Ueno T, et al. Comprehensive assay for the molecular profiling of cancer by target enrichment from formalin-fixed paraffin-embedded specimens. Cancer Sci 2019; 110: 1464-1479.

27. Boland CR, Thibodeau SN, Hamilton SR, et al. A National Cancer Institute Workshop on Microsatellite Instability for cancer detection and familial predisposition: development of international criteria for the determination of microsatellite instability in colorectal cancer. Cancer Res 1998; 58: 5248-5257.

28. Pardoll DM. The blockade of immune checkpoints in cancer immunotherapy. Nat Rev Cancer 2012; 12: 252-264.

29. Yang HM, Hsiao SJ, Schaeffer DF, et al. Identification of recurrent mutational events in anorectal melanoma. Mod Pathol 2017; 30: 286-296.

30. Maertens O, Johnson B, Hollstein P, et al. Elucidating distinct roles for NF1 in melanomagenesis. Cancer Discov. 2013;3: 338-49.

31. Hintzsche JD, Gorden NT, Amato CM, et al. Whole-exome sequencing identifies recurrent SF3B1 R625 mutation and comutation of NF1 and KIT in mucosal melanoma. Melanoma Res 2017; 27: 189-199.

32. Nissan MH, Pratilas CA, Jones AM, et al. Loss of NF1 in cutaneous melanoma is associated with RAS activation and MEK dependence. Cancer Res. 2014; 74: 2340-50.

33. Alsafadi S, Houy A, Battistella A, et al. Cancer-associated SF3B1 mutations affect alternative splicing by promoting alternative branchpoint usage. Nature communications 2016; 7: 10615.

34. Harbour JW, Roberson ED, Anbunathan H, Onken MD, Worley LA, Bowcock AM.

Recurrent mutations at codon 625 of the splicing factor SF3B1 in uveal melanoma. Nat Genet 2013; 45: 133-135.

35. Rivera RS, Nagatsuka H, Gunduz M, et al. C-kit protein expression correlated with activating mutations in KIT gene in oral mucosal melanoma. Virchows Arch 2008; 452: 27-32.

36. Antonescu CR, Busam KJ, Francone TD, et al. L576P KIT mutation in anal melanomas correlates with KIT protein expression and is sensitive to specific kinase inhibition. Int J Cancer 2007; 121: 257-264.

37. Montone KT, van Belle P, Elenitsas R, Elder DE. Proto-oncogene c-kit expression in malignant melanoma: protein loss with tumor progression. Mod Pathol 1997; 10: 939-944.

38. Hodi FS, Friedlander P, Corless CL, et al. Major response to imatinib mesylate in KIT-mutated melanoma. J Clin Oncol 2008; 26: 2046-2051.

39. Lutzky J, Bauer J, Bastian BC. Dose-dependent, complete response to imatinib of a metastatic mucosal melanoma with a K642E KIT mutation. Pigment cell & melanoma research 2008; 21: 492-493.

40. Guo J, Si L, Kong Y, et al. Phase II, open-label, single-arm trial of imatinib mesylate in patients with metastatic melanoma harboring c-Kit mutation or amplification. J Clin Oncol 2011; 29: 2904-2909

41. Lord CJ, Ashworth A. PARP inhibitors: Synthetic lethality in the clinic. Science 2017; 355: 1152-1158.

42. Yarchoan M, Hopkins A, Jaffee EM. Tumor Mutational Burden and Response Rate to PD-1 Inhibition. N Engl J Med 2017; 377: 2500-2501.

43. Rizvi NA, Hellmann MD, Snyder A, et al. Cancer immunology. Mutational landscape determines sensitivity to PD-1 blockade in non-small cell lung cancer. Science 2015; 348: 124-128.

44. Owada-Ozaki Y, Muto S, Takagi H, et al. Prognostic Impact of Tumor Mutation Burden in Patients With Completely Resected Non-Small Cell Lung Cancer: Brief Report. J Thorac Oncol 2018; 13: 1217-1221.

45. Madore J, Strbenac D, Vilain R, et al. PD-L1 Negative Status is Associated with Lower Mutation Burden, Differential Expression of Immune-Related Genes, and Worse Survival in Stage III Melanoma. Clin Cancer Res 2016; 22: 3915-392.

Figure legends

Fig. 1: Morphological features of PMME.

(A) Epithelioid pattern without rhabdoid pattern. (B) Papillary type. (C) Spindle type comprising spindle-shaped cells that proliferate in a fascicular pattern. (D) Rhabdoid pattern. Incohesive tumour cells with eosinophilic cytoplasm and eccentric nucleus are proliferating.

Fig. 2: Immunohistochemistry of c-kit, p53, and PD-L1.

Mainly cytoplasmic but focal membranous c-kit expression was observed in PMME #11 (A: HE, B: c-kit IHC). Diffuse p53 overexpression was observed in PMME #12 (C: HE, D: p53 IHC). This case harboured the *TP53* mutation. PD-L1 expression was detected in PMME #10 (E) and SKMM #9 (F).

Fig. 3: Survival rates in PMME.

(A) Three-year and five-year relapse-free survival rate was 23.1% and 7.7%, respectively. Median relapse-free survival rate was 7.2 months. (B) Three-year and five-year overall survival rate was 23.1% and 7.7%, respectively. Median survival rate was 11.9 months.

Fig. 4: Status of tumour mutation burden.

PMME showed significantly lower TMB compared with that of SKMM (p = 0.030 by Mann–Whitney U test).

Fig. 5: Supervised clustering based on the top 100 differentially expressed genes.

This analysis clearly distinguished between PMME and SKMM, except for one case (SKMM #1), suggesting that PMME is distinctively different from SKMM. Mutation profiles are also shown at the bottom.

Fig. 6: Supervised clustering based on RNA expression regarding T cell co-stimulator and co-inhibitor.

Both cases (PMME #10 and SKMM #9) with PD-L1 expression clustered within the same group. TMB level did not correlate with this grouping.

Table 1. Antibodies used for immunohistochemistry.

Antibody	Clone	Species	Source	Antigen retrieval	Dilution
AE1/AE3	AE1/AE3	Mouse Mono	DAKO	PK	x200
CAM5.2	CAM5.2	Mouse Mono	BD	PK	x10
c-kit	CD117	Rabbit Poly	DAKO	CB	x100
EMA	E29	Mouse Mono	Biogen	CB	x1 (predilution antibody)
Ki-67	MIB-1	Mouse Mono	DAKO	CB	x200
p53	1801	Mouse Mono	Biogen	TE	x1 (predilution antibody)

Abbreviation: Mono, monoclonal antibody; Poly, polyclonal antibody;
PK, proteinase K (10 min. at room temperature); CB, Citrate buffer (pH 6.0);
TE, Tris-EDTA Buffer (pH 9.0); BD, Becton, Dickinson and Company

Table 2. Clinicopathological findings in 13 PMME.

Age	mean 63.2 (range 47-74)
Sex	M:11, F:2
Location	Ut:1, Mt:7, Lt:3, EGJ:2
Macro	Type 0-Ip:6, 0-Is:2, 0-IIa+IIc:1, Type 1:3, Type 5:1
Size (mm)	mean 40.3 (range 21-58)
Depth of tumor invasion	M:1, SM:7, MP:5
lymphatic invasion	positive:4
vascular invasion	positive:6
N	positive:8
pStage (UICC 8th)	III:4, IVa:9
Survival periods (mos)	mean 29.8 (5.5-152.4)

Abbreviation: M, male; F, female;
Ut, upper thoracic esophagus; Mt, middle thoracic esophagus;
Lt, lower thoracic esophagus; EGJ, esophago-gastric junction;
M, mucosa; SM, submucosa; MP, muscularis propria

Table 3. Immunohistochemistry and molecular findings of 13 cases of PMMEs.

#	IHC						MSI status	Molecular finding				
	AE1/AE3	CAM5.2	EMA	p53	c-kit	PD-L1						
1	(-)	(-)	(-)	(-)	(-)	(-)	MSI-low	*SF3B1* p.Arg625His	*IGF1* p.Thr144Met			
2	(-)	(-)	(-)	(-)	(-)	(-)	MSS	N.A.				
3	(-)	(-)	(-)	(-)	(-)	(-)	MSI-low	N.A.				
4	(-)	(-)	(-)	(-)	(-)	(-)	MSI-low	*NF1* p.Gln2218fs	*RET* p.Gly691Ser	*ARID2* p.Lys179Arg	*FGFR4* p.Val262Met	*TMEM127* p.Ala132Thr
5	(-)	(-)	(-)	(+)	(-)	(-)	MSS	N.A.				
6	(-)	(-)	(-)	(+)	(-)	(-)	MSS	None				
7	(-)	(-)	(-)	(+)	(-)	(-)	MSS	*NF1* p.Ser536*	*CDKN2A* p.Phe90Leu	*MST1L* p.Pro642Leu		
8	(-)	(-)	(-)	(+)	(-)	(-)	MSS		*KRAS* p.Gly12Asp	*FMN2* p.Pro943Leu	*PTPRD* p.Met754Thr	
9	(-)	(-)	(-)	(+)	(-)	(-)	MSI-low	*NF1* p.Arg192fs	*SF3B1* p.Arg625His			
10	(-)	(-)	(-)	(+)	(-)	(+)	MSI-low	None				
11	(-)	(-)	(-)	(+)	(+)	(-)	MSS		*KIT* p.Asn822Tyr			
12	(-)	(-)	(-)	(++)	(-)	(-)	MSS		*TP53* p.Leu111Gln			
13	(-)	(-)	(-)	(+)	(-)	(-)	MSS		*BRCA2* p.Thr3033fs			

MSI, microsatellite instability; MSS, microsatellite stable; IHC, immunohistochemistry; N.A., not available

Fig.1

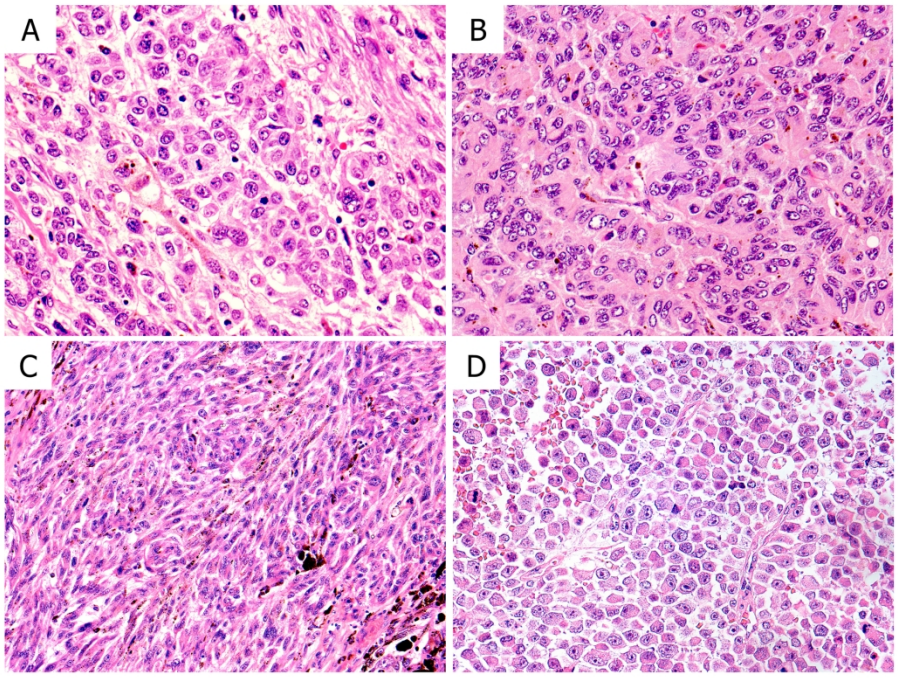

Fig.1

190x254mm (300 x 300 DPI)

Fig.2

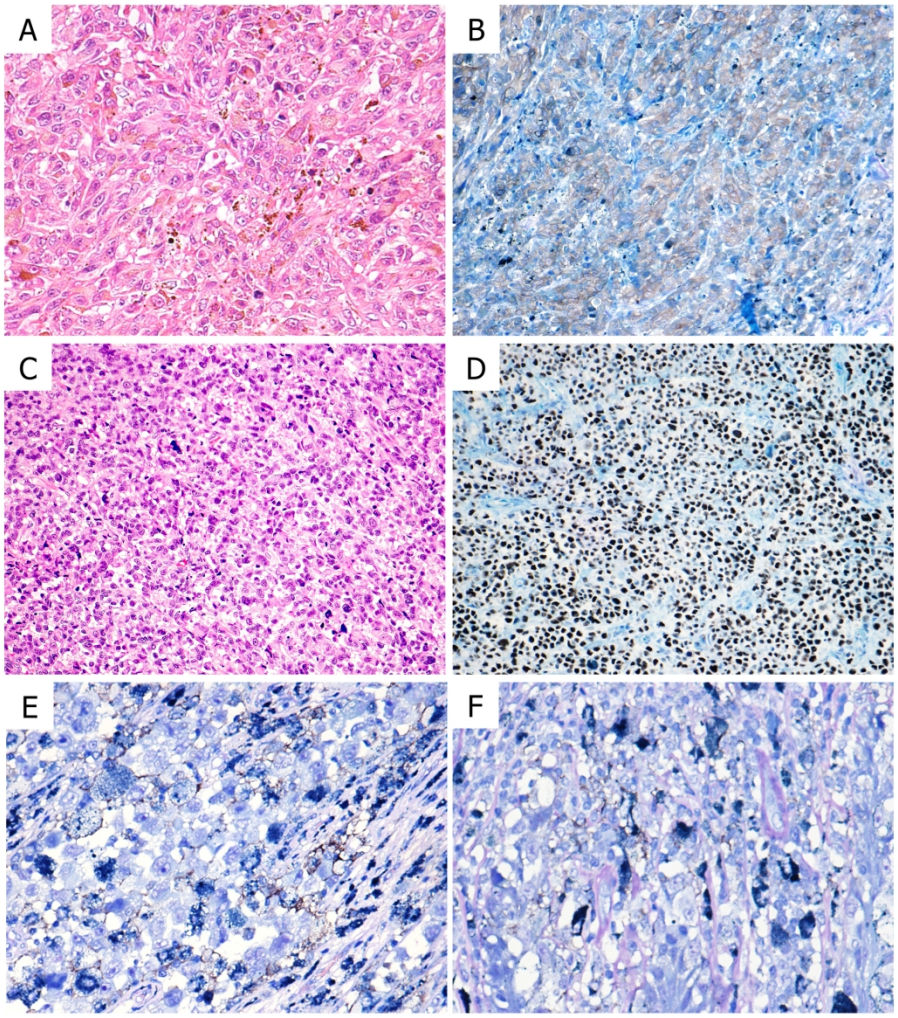

Fig.2

190x254mm (300 x 300 DPI)

Fig.3

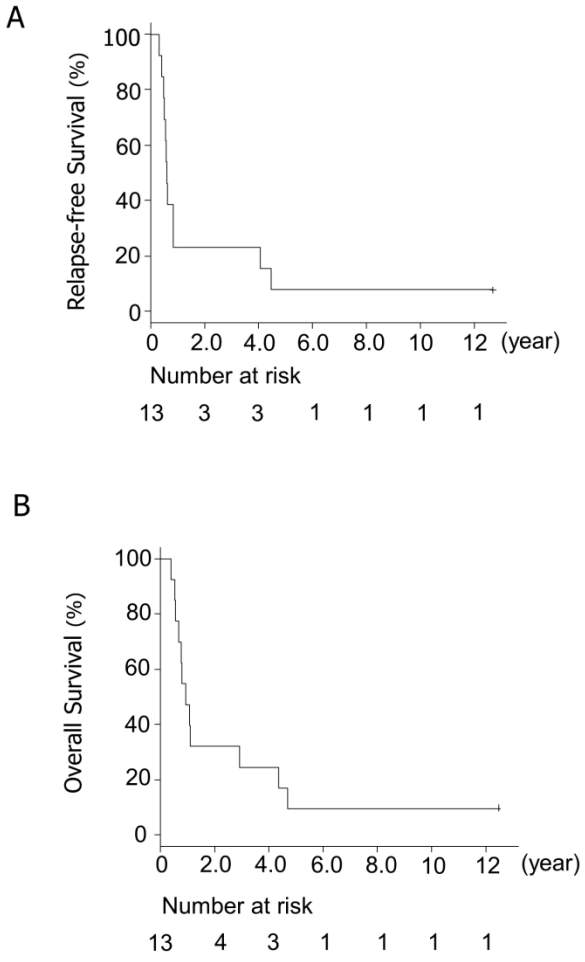

Fig.3

190x254mm (300 x 300 DPI)

Fig.4

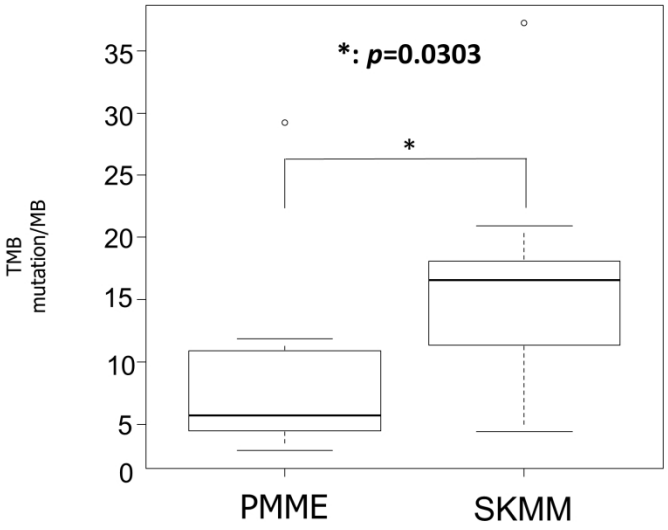

Fig.4

190x254mm (300 x 300 DPI)

Fig.5

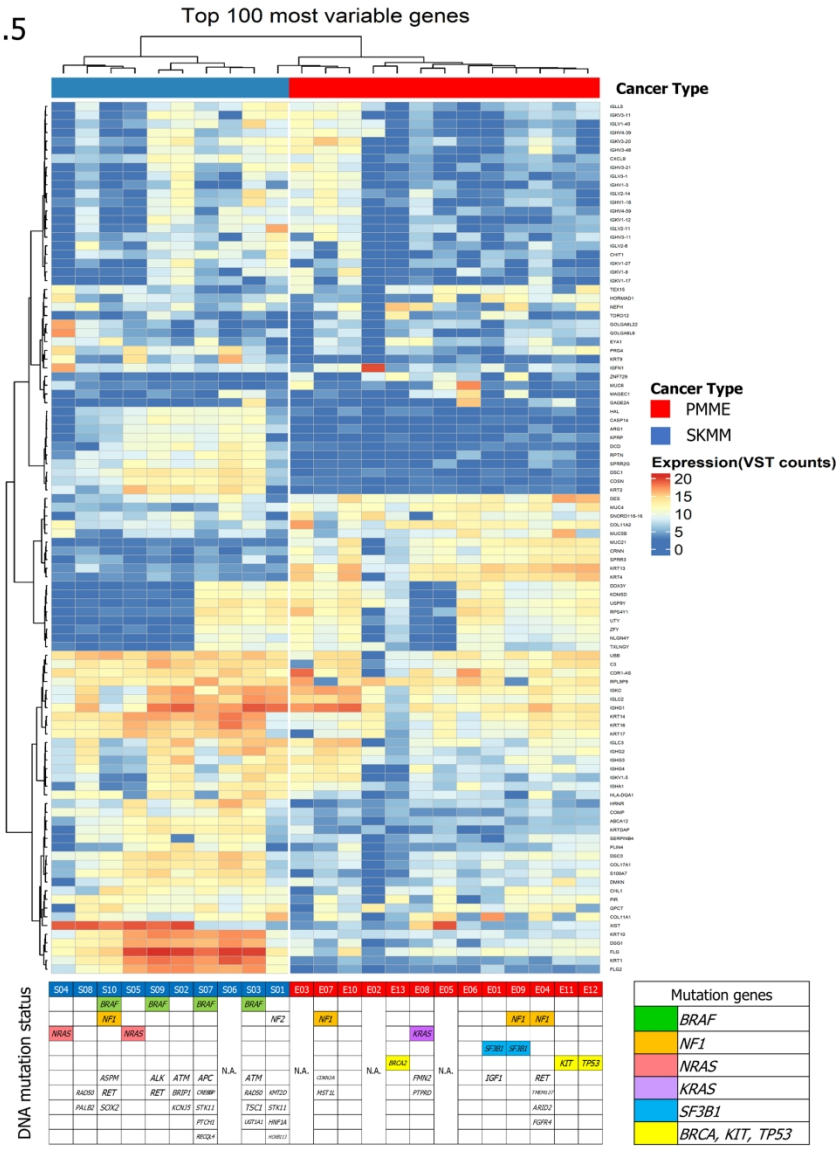

Fig.5

190x254mm (300 x 300 DPI)

Fig.6

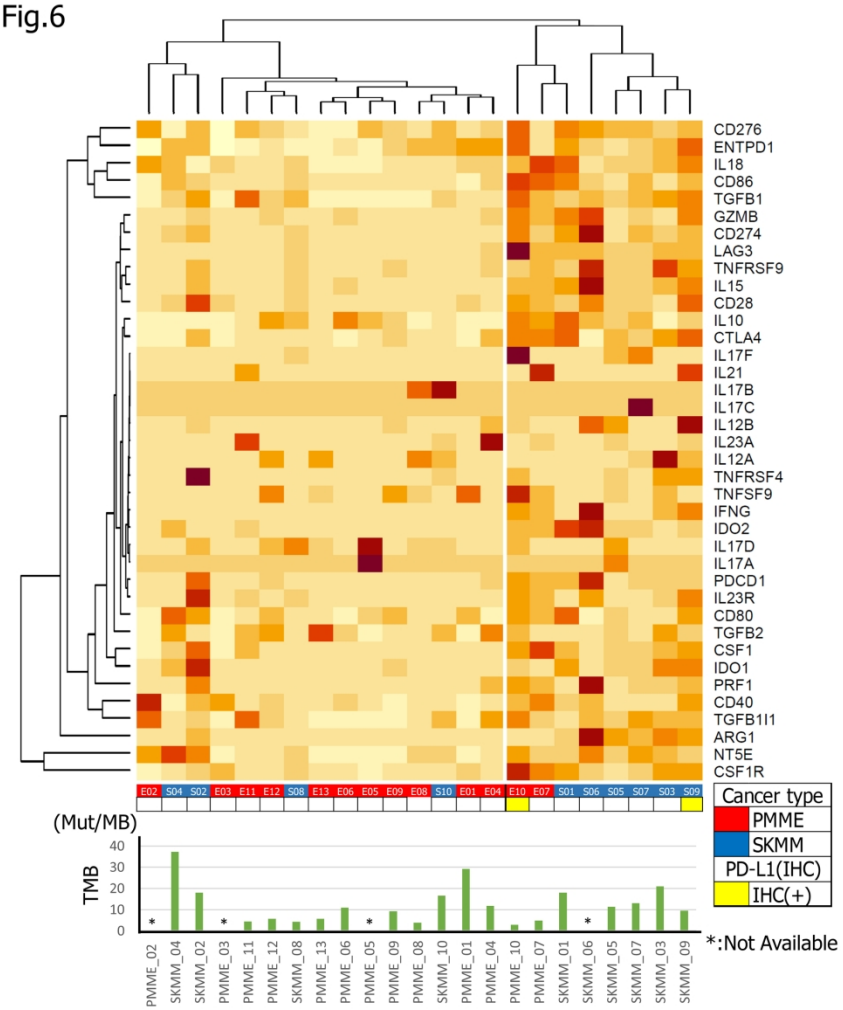

Fig.6

190x254mm (300 x 300 DPI)

Supplementary contents

Supplementary file Fig. 1. .tif (Supplementary Figure 1)

Legend for Supplementary Fig. 1:

(A) Overall survival rate with/without papillary feature. PMMEs with papillary structure tended to show better prognosis, but without a significant difference (p = 0.173).

(B) Overall survival rate according to *NF1* mutation status. *NF1* mutation positive patients tended to show better prognosis, but without a significant difference (p = 0.252).

Supplementary Table (Supplementary Table 1, Supplementary Table 2-1, Supplementary Table 2-2, Supplementary Table 3, Supplementary Table 4)

Supplementary Table 1. MSI evaluation.

Reference panel		
Marker	Repeating unit	GenBank accession No.
BAT25	Mononucleotide	9834508
BAT26	Mononucleotide	9834505
D2S123	Dinucleotide	187953
D5S346	Dinucleotide	181171
D17S250	Dinucleotide	177030

Supplementary Table 2-1. Clinicopathological features of PMME (13 cases)

#	Age	Sex	Location	Macro	Size(mm)	*in situ*	melanosis	epithelioid	rhabdoid	other features	melanocyte marker (IHC)			ly	v	Depth	pT(UICC8th)	pN(UICC8th)*	pStage(UICC8th)
											S-100	HMB-45	Melan A						
PMME_01	72	M	Lt	1	26	(+)	(+)	(+)	(-)		(+)	(+)	(+)	1	1	SM	T3	N0(0/101)	III
PMME_02	74	M	Lt	1	48	(+)	(-)	(-)	(-)	papillary	(+)	(+)	(+)	1	1	MP	T4a	N1(1/138)	IVA
PMME_03	63	M	EGJ	0-Is	48	(+)	(+)	(-)	(-)	papillary	(+)	(+)	(+)	1	1	MP	T4a	N0(0/53)	IVA
PMME_04	62	M	MtUt	0-Ip	58	(+)	(+)	(+)	(-)		(+)	(+)	(+)	1	1	M	T3	N1(3/105)	IVA
PMME_05	72	F	Mt	0-Ip	21	(+)	(+)	(+)	(+)		(+)	(+)	(+)	0	0	SM	T3	N0(0/77)	III
PMME_06	62	M	EGJ	0-Ip	24	(+)	(+)	(+)	(-)		(+)	(+)	(-)	0	0	SM	T3	N0(0/20)	III
PMME_07	63	M	Ut	1	27	(+)	(+)	(+)	(+)		(+)	(+)	(+)	0	1	SM	T3	N1(3/105)	IVA
PMME_08	64	F	Mt	0-Ip	50	(+)	(+)	(+)	(+)		(+)	(+)	(+)	0	0	SM	T3	N1(1/177)	IVA
PMME_09	47	M	MtLt	0-Ip	50	(+)	(+)	(+)	(-)	spindle, papillary	(+)	(+)	(+)	0	0	SM	T3	N1(7/137)	IVA
PMME_10	61	M	LtEGJ	5	50	(-)	(+)	(+)	(+)		(+)	(+)	(+)	0	0	MP	T4a	N1(4/41)	IVA
PMME_11	60	M	MtLt	0-Ip	40	(+)	(+)	(+)	(-)	spindle	(+)	(+)	(+)	0	0	MP	T4a	N1(2/70)	IVA
PMME_12	51	M	Mt	0-IIa+IIc	52	(+)	(+)	(+)	(+)		(+)	(+)	(+)	0	0	MP	T4a	N1(1/144)	IVA
PMME_13	71	M	Mt	0-Is	30	(+)	(+)	(+)	(+)		(+)	(+)	(+)	0	1	SM	T3	N0(0/73)	III

Abbreviations: Ut, upper thoracic esophagus; Mt, middle thoracic esophagus; Lt, lower thoracic esophagus; EGJ, esophago-gastric junction; IHC, Immunohistochemistry

ly, lymphatic invasion; v, vascular invasion; M, mucosa; SM, submucosa; MP, muscularis propria; T, depth of tumor invasion; N, lymph node metastasis; UICC, The Union for International Cancer Control

DOD, dead of disease; LOST, lost to follow-up; NED, no evidence of disease; NAC, neoadjuvant chemotherapy; CT, chemotherapy; RT, radiation therapy; CRT, chemoradiation therapy

DAV, dacarbazine+nimustine+vincristine; DAC-tam, dacarbazine+nimustine+cisplatin+tamoxifen.

* the denominator is the number of resected lymph node and numerator is the number of metastasis of lymph nodes.

Supplementary Table 2-2. Clinicopathological features of PMME (13 cases). (continued)

#	Distant metastasis	Up to recurrece (mos.)	Prognosis	Survival period (mos.)	Additional therapy
PMME_01	liver	5.0	DOD	5.5	none
PMME_02	lung	53.8	DOD	57.4	unknown
PMME_03	abdomen	48.8	DOD	53.3	DAC-tam, DAV
PMME_04	bone, lymph node (neck)	10.0	DOD	11.9	NAC(DAC-Tam), CRT(DAV-Tam+S-1+RT(48Gy))
PMME_05	none	-	NED+LOST	152.4	none
PMME_06	pleura	7.2	DOD	13.7	RT, DAV
PMME_07	lung	6.4	DOD	10.0	CRT
PMME_08	peritoneum	5.8	DOD	8.8	NAC(DAV)
PMME_09	lymph node (paraaorta)	6.7	DOD	36.0	NAC(DAV), DAC-Tam, Paclitaxel+Carboplatin
PMME_10	abdomen, neck, skin	10.0	DOD	10.4	NAC(CRT), DAV, OK432
PMME_11	lung, liver, lymph node, eye	5.9	DOD	7.3	none
PMME_12	adrenal glands, bone, skin, lymph node (peritoneum)	7.2	DOD	13.9	OK432, RT(39Gy)
PMME_13	pleura, lymph node	3.6	DOD	7.2	RT(39Gy)+S-1, Nivolumab

Abbreviations: DOD, dead of disease; LOST, lost to follow-up; NED, no evidence of disease
CRT, chemoradiation therapy; NAC, neoadjuvant chemoterapy; CT, chemotherapy; RT, radiation therapy
DAV, dacarbazine; DAC-tam, dacarbazine+nimustine+cisplatin+tamoxifen

Supplementary Table 3. Clinicopathological features of skin malignant melanoma (10 cases).

#	Age	Sex	Location	subtype	Size(mm)	Breslow depth (mm)	Clark level	UL	T	pN(UICC8th)	pStage(UICC8th)	Survival period (mos.)	Distant metastasis	Prognosis
SKMM_01	65	M	Neck	cutaneous	45x49	12	IV	(-)	T4a	N1	IIIC	83.0	brain, lung	dead of disease
SKMM_02	55	F	Thigh	cutaneous	35x23	18	IV	(-)	T4a	N2a	IIIC	120.0		no recurrence
SKMM_03	44	M	Thigh	cutaneous	35x25	4.5	IV	(+)	T4b	N1	IIIC	46.3		no recurrence
SKMM_04	71	F	Sole	acral	30x15	17	V	(+)	T4b	N0	IIC	20.0	lung, peritoneum	dead of disease
SKMM_05	84	F	Sole	acral	17x15	4	V	(+)	T4b	N0	IIA	76.9	thigh	recurrence
SKMM_06	79	M	Sole	acral	32x30	3	IV	(-)	T3a	N0	IIB	25.5	unkown	dead
SKMM_07	67	M	Lumbar	cutaneous	30x20	3.5	IV	(+)	T3b	N0	IIC	40.4	lung, bone, brain	dead of disease
SKMM_08	68	F	Vulva	cutaneous	28x19	24	V	(+)	T4b	N0	IIB	46.7	skin, pancreas	recurrence
SKMM_09	53	F	Upper arm	cutaneous	15x15	4.5	IV	(-)	T4a	N0	IIB	22.9		no recurrence
SKMM_10	51	F	Forearm	cutaneous	15x11	4.8	IV	(+)	T4b	N0	IIC	23.4	lymph node	recurrence

Abbreviations: UL, ulcer; T, depth of tumor invasion; ly, lymphatic invasion; v, vascular invasion

Supplementary Table 4. Genetic alterations in skin malignant melanoma.

#	Genetic alteration						IHC
SKMM_01			*NF2* p.Arg466*	*KMT2D* p.Arg5224His	*STK11* p.Phe354Leu	*HNF1A* p.Ala568Thr	*HOXB13* p.Ala212Thr	
SKMM_02			*ATM* p.Thr935Arg	*BRIP1* p.Asn852Asp	*KCNJ5* p.Gly387Arg			
SKMM_03	*BRAF* p.Val600Glu		*ATM* p.Thr935Arg	*RAD50* p.Leu1264Phe	*TSC1* p.Gln654Glu	*UGT1A1* p.Gly71Arg		
SKMM_04		*NRAS* p.Gln61Lys						
SKMM_05		*NRAS* p.Gln61Arg						
SKMM_06				N.A.				
SKMM_07	*BRAF* p.Val600Glu		*APC* p.Arg2525His	*CREBBP* p.Leu551Ile	*STK11* p.Phe354Leu	*PTCH1* p.Arg893His	*RECQL4* p.Arg43Trp	
SKMM_08			*PALB2* p.Tyr743Cys	*RAD50* p.Thr1127Ile				
SKMM_09	*BRAF* p.Val600Glu		*ALK* p.Thr1087Ile	*RET* p.Gly691Ser				PD-L1(+)
SKMM_10	*BRAF* p.Val600Glu		*NF1* p.Pro2782Thr	*RET* p.Gly691Ser	*SOX2* p.Asn46Lys	*ASPM* p.Ile313Val		

Abbreviations: N.A., not available; IHC, immunohistochemistry

Suppl. Fig.1

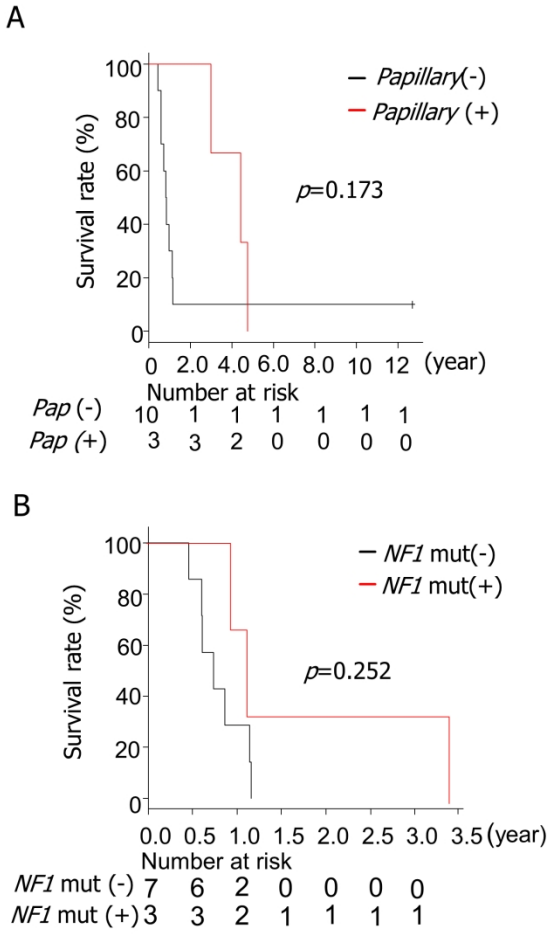

190x254mm (300 x 300 DPI)